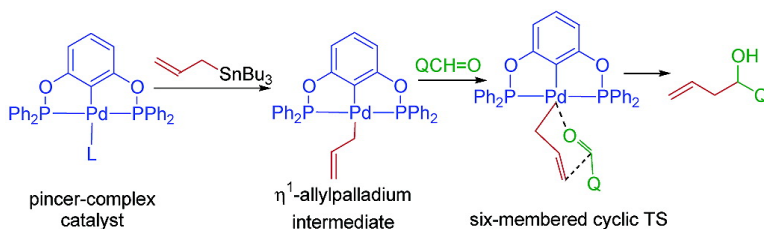


## Pincer Complex-Catalyzed Allylation of Aldehyde and Imine Substrates via Nucleophilic $\eta^1$ -Allyl Palladium Intermediates

Niclas Solin, Johan Kjellgren, and Klmn J. Szab

*J. Am. Chem. Soc.*, **2004**, 126 (22), 7026-7033 • DOI: 10.1021/ja049357j • Publication Date (Web): 08 May 2004

Downloaded from <http://pubs.acs.org> on March 31, 2009



### More About This Article

Additional resources and features associated with this article are available within the HTML version:

- Supporting Information
- Links to the 12 articles that cite this article, as of the time of this article download
- Access to high resolution figures
- Links to articles and content related to this article
- Copyright permission to reproduce figures and/or text from this article

[View the Full Text HTML](#)



## Pincer Complex-Catalyzed Allylation of Aldehyde and Imine Substrates via Nucleophilic $\eta^1$ -Allyl Palladium Intermediates

Niclas Solin, Johan Kjellgren, and Kálmán J. Szabó\*

Contribution from the Arrhenius Laboratory, Department of Organic Chemistry, Stockholm University, SE-106 91 Stockholm, Sweden

Received February 5, 2004; E-mail: kalman@organ.su.se

**Abstract:** Electrophilic allylic substitution of allylstannanes with aldehyde and imine substrates could be achieved by employment of palladium pincer complex catalysts. It was found that the catalytic activity of the pincer complexes is highly dependent on the ligand effects. The best results were obtained by employment of PCP pincer complexes with weakly coordinating counterions. In contrast to previous applications for electrophilic allylic substitutions via bisallylpalladium complexes, the presented reactions involve monoallylpalladium intermediates. Thus, employment of pincer complex catalysts extends the synthetic scope of the palladium-catalyzed allylic substitution reactions. Moreover, use of these catalysts eliminates the side reactions occurring in transformations via bisallylpalladium intermediates. The key intermediate of the electrophilic substitution reaction was observed by  $^1\text{H}$  NMR spectroscopy. This intermediate was characterized as an  $\eta^1$ -allyl-coordinated pincer complex. Density functional theory (DFT) modeling shows that the electrophilic attack can be accomplished with a low activation barrier at the  $\gamma$ -position of the  $\eta^1$ -allyl moiety. According to the DFT calculations, this reaction takes place via a six-membered cyclic transition-state (TS) structure, in which the tridentate coordination state of the pincer ligand is preserved. The stereoselectivity of the reaction could be explained on the basis of the six-membered cyclic TS model.

### 1. Introduction

Palladium-catalyzed allylic substitution reactions via allylpalladium intermediates represent one of the most important procedures in modern organic synthesis.<sup>1,2</sup> Palladium-catalyzed allylic displacement of acetate, carbonate, and their congeners with nucleophilic reagents has become a very important and versatile synthetic procedure. This nucleophilic substitution reaction involves oxidative addition of palladium(0) to the allylic substrate, generating an  $\eta^3$ -(mono)allylpalladium intermediate followed by a nucleophilic attack, providing the allylated product and regenerating the palladium(0) catalyst.<sup>1,2</sup>

Possibilities to extend the synthetic scope of the palladium-catalyzed allylic substitutions to *electrophilic* substrates have recently been the subject of a great deal of interest in mechanistic and in synthetic organic chemistry.<sup>3–12</sup> In the commonly used

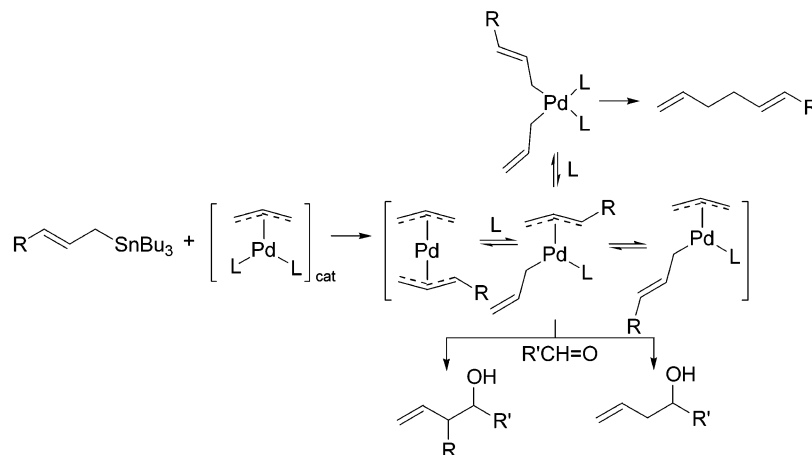
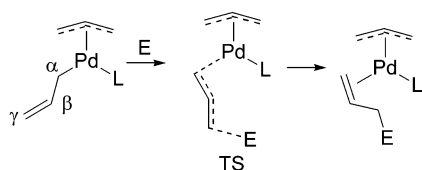
version of these reactions, the key step involves *electrophilic* attack on a bisallylpalladium complex (Scheme 1), which can be generated from a monoallylpalladium complex and allylstannane.<sup>3,13</sup> Subsequently, this bisallylpalladium complex reacts with an electrophile, affording the allylated product and the regenerated catalyst.<sup>3</sup> An important application of this transformation involves enantioselective allyl transfer via chiral allylpalladium complexes.<sup>4,7</sup>

Theoretical studies revealed that the electrophilic attack proceeds via an  $\eta^1, \eta^3$ -bisallylpalladium species formed from the  $\eta^3, \eta^3$ -form by ligand coordination (Scheme 2).<sup>14</sup> The electrophilic attack takes place at the  $\gamma$ -position of the  $\eta^1$ -moiety with a remarkably low activation barrier. It was also concluded that the other  $\eta^3$ -coordinated allyl group acts as an electron-supplying spectator ligand. Accordingly, the spectator ligands (the  $\eta^3$  moiety and L) together occupy three of the four coordination sites on palladium.

In the traditionally used version of the electrophilic substitution reactions, formation of various isomeric bisallylpalladium complexes with different reactivities (Scheme 1) imposes considerable limitations on the synthetic scope of the catalytic transformation. Catalytic formation of unsymmetrically substituted  $\eta^3, \eta^3$ -bisallylpalladium complexes ( $R \neq H$ , Scheme 1) involves generation of various  $\eta^1, \eta^3$ -intermediates, and therefore, either allyl group can be transferred to the electrophile.<sup>8,9</sup> Control

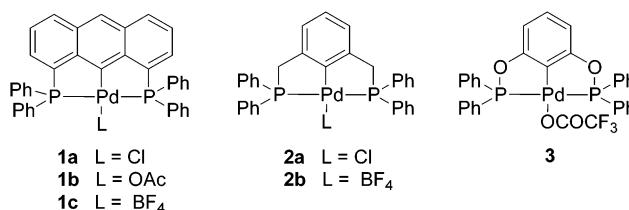
- (1) Tsuji, J. *Perspectives in Organopalladium Chemistry for the 21st Century*; Elsevier: Amsterdam, 1999.
- (2) Tsuji, J. *Palladium Reagents and Catalysis: Innovations in Organic Synthesis*; Wiley: Chichester, U.K., 1995.
- (3) Nakamura, H.; Iwama, H.; Yamamoto, Y. *J. Am. Chem. Soc.* **1996**, *118*, 6641.
- (4) Nakamura, H.; Nakamura, K.; Yamamoto, Y. *J. Am. Chem. Soc.* **1998**, *120*, 4242.
- (5) Nakamura, H.; Shim, J.-G.; Yamamoto, Y. *J. Am. Chem. Soc.* **1997**, *119*, 8113.
- (6) Nakamura, H.; Aoyagi, K.; Shim, J.-G.; Yamamoto, Y. *J. Am. Chem. Soc.* **2001**, *123*, 372.
- (7) Fernandes, R. A.; Stimac, A.; Yamamoto, Y. *J. Am. Chem. Soc.* **2003**, *125*, 14133.
- (8) Solin, N.; Narayan, S.; Szabó, K. J. *J. Org. Chem.* **2001**, *66*, 1686.
- (9) Solin, N.; Narayan, S.; Szabó, K. J. *Org. Lett.* **2001**, *3*, 909.
- (10) Wallner, O. A.; Szabó, K. J. *Org. Lett.* **2002**, *4*, 1563.
- (11) Wallner, O. A.; Szabó, K. J. *J. Org. Chem.* **2003**, *68*, 2934.

- (12) Wallner, O. A.; Szabó, K. J. *Chem. Eur. J.* **2003**, *9*, 4025.
- (13) Goliaszewski, A.; Schwartz, J. *Tetrahedron* **1985**, *41*, 5779.
- (14) Szabó, K. J. *Chem. Eur. J.* **2000**, *6*, 4413.

**Scheme 1.** Formation, Reactivity, and Isomerization Possibilities of Bisallylpalladium Intermediates**Scheme 2.** Mechanism of the Electrophilic Attack at the  $\eta^1$ -Allyl Moiety of an  $\eta^3, \eta^3$ -Bisallylpalladium Complex

of the regioselectivity is a particularly important issue in asymmetric applications,<sup>4,7</sup> where the electrophilic attack on the chiral allyl moiety must be avoided to maintain the asymmetric activity of the allylpalladium catalyst. A further important problem is that bisallylpalladium complexes may undergo allyl-allyl (Stille) coupling instead of reaction with electrophiles.<sup>13,15–17</sup> This reaction particularly easily occurs in the presence of excessive amounts of strongly coordinating ligands (L, Scheme 1), which promotes the formation of the  $\eta^1, \eta^1$ -bisallylic isomer. Echavarren and Cárdenas and co-workers<sup>17</sup> have recently shown that  $\eta^1, \eta^1$ -bisallylpalladium complexes easily undergo reductive elimination to give 1,5-hexadiene derivatives.

Accordingly, a further innovative development of the palladium-catalyzed electrophilic substitution reactions requires that the catalytic transformations do proceed entirely via monoallylpalladium intermediates without involvement of bisallylpalladium species. However, development of such catalytic transformations poses a great challenge, since the usual monoallylpalladium complexes are considerably more stable as  $\eta^3$ -coordinated species<sup>18</sup> (in which the allyl moiety has an electrophilic character) than in their  $\eta^1$ -coordinated forms required in the electrophilic attack (Scheme 2). Therefore, the spectator ligand in a monoallylpalladium complex reactive toward electrophiles has to fulfill at least four important criteria: (a) The spectator ligand has to perform a tridentate coordination to palladium. Thus only one free coordination site will be available on palladium to ensure  $\eta^1$ -coordination of the allyl moiety. (b) A strong electron donor ability is required to lend a nucleophilic character to the allyl group. (c) A firm palladium–ligand bonding is necessary to avoid undesired dynamic processes and ligand exchange. (d) The electron-supplying part of the spectator

**Chart 1.** Studied Active Pincer Complex Catalysts

ligand must be forced to a trans position relative to the allyl ligand in order to avoid reductive coupling (cf. Stille coupling) between the spectator ligand and the allyl moiety.

As we have shown in a recent paper, the above requirements can be fulfilled by application of PCP- (**1–2**) type pincer complexes in the catalytic electrophilic substitution reactions.<sup>19</sup> These type of pincer complexes are characterized by strong tridentate ligand coordination and direct aryl–metal bonding, which provides an electron-rich palladium atom (Chart 1).<sup>20–26</sup> In this paper we give a full account of our results on pincer complex-catalyzed electrophilic substitution reactions. In addition, we present our new studies on some important synthetic and mechanistic aspects of this reaction: (i) possibilities to improve the catalytic activity of the applied pincer catalysts (cf. **3**); (ii) direct observation of the allylpalladium intermediate of the reaction to assess the reaction mechanism; and (iii) modeling the electrophilic attack on the allylic moiety of the pincer complex intermediate of the reaction by density functional theory (DFT).

## 2. Catalytic Electrophilic Substitution by Pincer Complexes

As we communicated before,<sup>19</sup> PCP pincer complexes **1** and **2** are able to catalyze the electrophilic substitution of allylstan-

(15) Golaszewski, A.; Schwartz, J. *J. Am. Chem. Soc.* **1984**, *106*, 5028.  
 (16) Nakamura, H.; Bao, M.; Yamamoto, Y. *Angew. Chem., Int. Ed.* **2001**, *40*, 3208.  
 (17) Méndez, M.; Cuerva, J. M.; Gómez-Bengoa, E.; Cárdenas, D. J.; Echavarren, A. M. *Chem. Eur. J.* **2002**, *8*, 3620.  
 (18) Solin, N.; Szabó, K. *J. Organometallics* **2001**, *20*, 5464.

(19) Solin, N.; Kjellgren, J.; Szabó, K. *J. Angew. Chem., Int. Ed.* **2003**, *42*, 3656.  
 (20) Albrecht, M.; Kotten, G. v. *Angew. Chem., Int. Ed.* **2001**, 3750.  
 (21) Singleton, J. T. *Tetrahedron* **2003**, *59*, 1837.  
 (22) Rimmli, H.; Venanzi, L. M. *J. Organomet. Chem.* **1983**, 259, C6.  
 (23) Haenel, M. W.; Oevers, S.; Bruckmann, J.; Kuhnigk, J.; Krüger, C. *Synlett* **1998**, 301.  
 (24) Haenel, M. W.; Jakubik, D.; Krüger, C.; Betz, P. *Chem. Ber.* **1991**, *124*, 333.  
 (25) Beek, J. A. M. v.; Kotten, G. v.; Dekker, G. P. C. M.; Wissing, E.; Zoutberg, M. C.; Stam, C. H. *J. Organomet. Chem.* **1990**, 394, 659.  
 (26) Slagt, M. Q.; Rodríguez, G.; Grutters, M. M. P.; Gebbink, R. J. M. K.; Klopper, W.; Jenneskens, L. W.; Lutz, M.; Spek, A. L.; Kotten, G. v. *Chem. Eur. J.* **2004**, *10*, 1331.

**Table 1.** Pincer Complex-Catalyzed<sup>a</sup> Electrophilic Substitution Reactions

entry	substrate 1	substrate 2	cat.	prod.	Q	R <sup>1</sup>	solvent	conditions <sup>b</sup>	yield <sup>c</sup>
1	<b>4a</b>	<b>5a</b>	<b>1a</b>	<b>7a</b>	C <sub>6</sub> H <sub>5</sub>	H	DMF	60/22	81
2	<b>4a</b>	<b>5a</b>	<b>2a</b>	<b>7a</b>	C <sub>6</sub> H <sub>5</sub>	H	THF	60/21	88
3	<b>4a</b>	<b>5a</b>	<b>3</b>	<b>7a</b>	C <sub>6</sub> H <sub>5</sub>	H	THF	40/18	92
4	<b>4a</b>	<b>5b</b>	<b>1a</b>	<b>7b</b>	4-CN-C <sub>6</sub> H <sub>5</sub>	H	DMF	60/17	88
5	<b>4a</b>	<b>5c</b>	<b>1a</b>	<b>7c</b>	4-CH <sub>3</sub> CO-C <sub>6</sub> H <sub>5</sub>	H	DMF	60/17	82
6	<b>4a</b>	<b>5c</b>	<b>3</b>	<b>7c</b>	4-CH <sub>3</sub> CO-C <sub>6</sub> H <sub>5</sub>	H	THF	25/15	95
7	<b>4a</b>	<b>5d</b>	<b>1a</b>	<b>7d</b>	4-NO <sub>2</sub> -C <sub>6</sub> H <sub>5</sub>	H	DMF	60/17	82
8	<b>4a</b>	<b>5d</b>	<b>1b</b>	<b>7d</b>	4-NO <sub>2</sub> -C <sub>6</sub> H <sub>5</sub>	H	CHCl <sub>3</sub>	40/2	95
9	<b>4a</b>	<b>5d</b>	<b>1c</b>	<b>7d</b>	4-NO <sub>2</sub> -C <sub>6</sub> H <sub>5</sub>	H	CHCl <sub>3</sub>	20/3	95
10	<b>4a</b>	<b>5d</b>	<b>2a</b>	<b>7d</b>	4-NO <sub>2</sub> -C <sub>6</sub> H <sub>5</sub>	H	THF	40/21	95
11	<b>4a</b>	<b>5d</b>	<b>3</b>	<b>7d</b>	4-NO <sub>2</sub> -C <sub>6</sub> H <sub>5</sub>	H	THF	25/3	95
12	<b>4a</b>	<b>5e</b>	<b>2a</b>	<b>7e</b>	cinnamyl	H	THF	60/21	80
13	<b>4a</b>	<b>5e</b>	<b>3</b>	<b>7e</b>	cinnamyl	H	THF	40/24	80
14	<b>4a</b>	<b>5f</b>	<b>3</b>	<b>7f</b>	hexyl	H	THF	60/28	73
15	<b>4a</b>	<b>5g</b>	<b>3</b>	<b>7g</b>	cyclohexyl	H	THF	60/26	72
16	<b>4a</b>	<b>6</b>	<b>1a</b>	<b>8a</b>		H	DMF	60/17	66
17	<b>4a</b>	<b>6</b>	<b>2a</b>	<b>8a</b>		H	THF	60/21	69
18	<b>4a</b>	<b>6</b>	<b>3</b>	<b>8a</b>		H	THF	40/16	95
19	<b>4b</b>	<b>5a</b>	<b>2a</b>	<b>7h</b>	C <sub>6</sub> H <sub>5</sub>	Ph	THF	60/21	61 <sup>d</sup>
20	<b>4b</b>	<b>5d</b>	<b>2a</b>	<b>7i</b>	4-NO <sub>2</sub> -C <sub>6</sub> H <sub>5</sub>	Ph	THF	60/21	95 <sup>d</sup>
21	<b>4b</b>	<b>5d</b>	<b>15</b>	<b>7i</b>	4-NO <sub>2</sub> -C <sub>6</sub> H <sub>5</sub>	Ph	THF	20/64	85 <sup>d</sup>
22	<b>4b</b>	<b>5g</b>	<b>3</b>	<b>7j</b>	cyclohexyl	Ph	THF	60/40	49 <sup>e</sup>
23	<b>4c</b>	<b>5d</b>	<b>1a</b>	<b>7k</b>	4-NO <sub>2</sub> -C <sub>6</sub> H <sub>5</sub>	Me	DMF	60/14	77 <sup>e</sup>
24	<b>4d</b>	<b>5d</b>	<b>3</b>	<b>7k</b>	4-NO <sub>2</sub> -C <sub>6</sub> H <sub>5</sub>	Me	THF	40/14	65 <sup>e</sup>
25	<b>4d</b>	<b>5a</b>	<b>3</b>	<b>7l</b>	C <sub>6</sub> H <sub>5</sub>	Me	THF	60/40	57 <sup>e</sup>
26	<b>4b</b>	<b>6</b>	<b>2a</b>	<b>8b</b>		Ph	THF	60/21	65 <sup>h</sup>

<sup>a</sup> Catalyst (5 mol %) was applied. <sup>b</sup> Temperature (°C)/time (h). <sup>c</sup> Isolated yield. <sup>d</sup> Diastereomer ratio anti/syn<sup>28</sup> = 10:1. <sup>e</sup> Diastereomer ratio anti/syn<sup>29</sup> = 14:1. <sup>f</sup> Z/E ratio = 2:1. <sup>g</sup> Diastereomer ratio syn/anti<sup>30</sup> = 1:1. <sup>h</sup> Diastereomer ratio syn/anti<sup>31</sup> = 12:1.

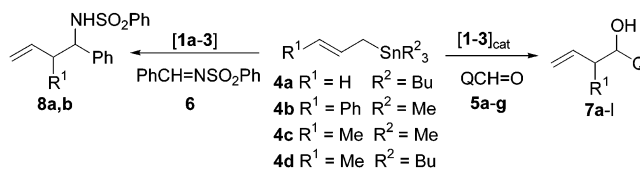
nanes **4a–c** with aldehyde (**5a–e**) and imine (**6**) electrophiles. By use of 5 mol % catalyst **1a** and **2a**, a typical reaction was conducted at 60 °C overnight to obtain a full conversion of the reactants (Scheme 3).

All reactions proceed under neutral conditions, and therefore many functionalities such as the cyano (entry 4), keto (entry 5), and nitro (entries 7–10) groups are tolerated (Table 1). The high chemoselectivity of the reaction was demonstrated by allylation of keto aldehyde **5c** (entry 5). In this process the aldehyde functionality could be allylated, while the keto group remained unchanged.

We have also studied the regio- and stereoselectivity of the reaction. It was found that cinnamyl stannane (**4b**) readily undergoes palladium-catalyzed allylic substitution with aldehydes **5a** and **5d**, providing exclusively the branched allylic products (**7h** and **7i**) with high anti diastereoselectivity (entries 19 and 20). Sulfonimine **6** and stannane **4b** also react with the same regioselectivity and with a high stereoselectivity (entry 26). Interestingly, in this reaction the major stereoisomer is the syn form. The catalytic substitution reaction with crotyl stannane (**4c**) also gives the branched allylic isomer (**7k**); however, the two diastereomers form in a 1:1 ratio (entry 23).

We attempted to increase the catalytic activity of the pincer complexes by replacement of the strongly coordinating chloride counterion with acetate and tetrafluoroborate (e.g., **1b,c**).<sup>27</sup> Comparison of entry 7 with entries 8 and 9 clearly indicate that acetate complex **1b** and tetrafluoroborate complex **1c** are more reactive catalysts than chloro complex **1a**. With catalytic amounts of **1b** and **1c**, the reaction with nitrobenzaldehyde (**5d**)

(27) Complexes **1b,c** and **2b** were generated from **1a** and **2a**, respectively. The corresponding chloro complex was dissolved in CHCl<sub>3</sub>, mixed with AgBF<sub>4</sub> (**1b** and **2b**) or AgOAc (**1c**) at room temperature, and then the mixture was stirred for 30 min. The precipitate was removed and the resulting clear solution was used without further purification.

**Scheme 3.** Pincer Complex-Catalyzed Electrophilic Substitution Reactions

was complete in a couple of hours at room temperature or at 40 °C. However, the acetate and tetrafluoroborate complexes were rapidly deactivated under the applied catalytic conditions. Therefore, these catalysts could not be employed for allylation of nonactivated aldehydes (such as **5a** and **5f,g**) requiring a longer reaction time.

**Increase of the Catalytic Activity by Employment of Complex 3.** Since we found that the catalytic activity of pincer complexes with weakly coordinating counterions is higher than with chloride counterion, we considered using trifluoroacetate complex **3** as a catalyst in the electrophilic allylic substitution reactions. This pincer complex is readily available by a two-step synthesis reported by Bedford et al.<sup>32</sup> Complex **3** is highly stable under the applied reaction conditions and its catalytic activity is preserved at least for 24 h even at 60 °C.

As expected, trifluoroacetate complex **3** outperforms chloro complexes **1a** and **2a** in all catalytic reactions. Thus benzaldehyde (**5a**) was allylated at 40 °C in excellent yield with **3** as a catalyst (entry 3), while the reaction with complexes **1a** and **2a** had to be conducted at 60 °C and for a longer time (entries 1 and 2). Furthermore, allylation of aldehyde **5c** was performed at room temperature with **3** (entry 6), while 60 °C reaction temperature was required for the same process catalyzed by **1a** (entry 5). By employment of **3**, nitrobenzaldehyde (**5d**) could be allylated at about the same temperature and in the same reaction time (entry 11) as with tetrafluoroborate complex **1c**. Not only benzaldehyde derivatives but also cinnamyl aldehyde (**5e**) (cf. entries 12 and 13) and benzenesulfonimine (**6**) (cf. entries 16–17 and 18) reacted faster with **4a** in the presence of **3** than with catalytic amounts of **1a** and **2a**. Most importantly, electrophilic substitution of allylstannane **4a** with aliphatic aldehydes **5f,g** could be achieved with high yields by employment of catalyst **3** (entries 14 and 15), while the same catalytic reaction with **1** and **2** resulted in only traces of products under similar or even under harsh reaction conditions. Cinnamylstannane **4b** could also be reacted with **5g**, affording cyclohexyl derivative **7j** in a moderate yield and with excellent stereo- and regioselectivity (entry 22). Crotylstannanes (**4c,d**) react much slower with aldehydes than the parent allylstannane (**4a**). Crotyltributylstannane (**4d**) reacts very slowly with **5d** even at 60 °C in the presence of **1a**. Therefore, we employed crotyltrimethylstannane (**4c**) to accomplish this reaction (entry 23). However, in the presence of the highly active catalyst **3**, stannane **4c** could be replaced by the less reactive substrate **4d**, and moreover, the reaction temperature was decreased to 40 °C (entry 24). Even catalytic coupling of benzaldehyde (**5a**)

(28) Takahara, J. P.; Masuyama, Y.; Kurusu, Y. *J. Am. Chem. Soc.* **1992**, *114*, 2577.

(29) Loh, T.-P.; Tan, K.-T.; Hu, Q.-Y. *Angew. Chem., Int. Ed.* **2001**, *40*, 2921.

(30) Batey, R. A.; Thadani, A. N.; Smil, D. V.; Lough, A. J. *Synthesis* **2000**, 990.

(31) Lu, W.; Chan, T. H. *J. Org. Chem.* **2000**, *65*, 8589.

(32) Bedford, R. B.; Draper, S. M.; Scully, P. N.; Welch, S. L. *New J. Chem.* **2000**, *24*, 745.

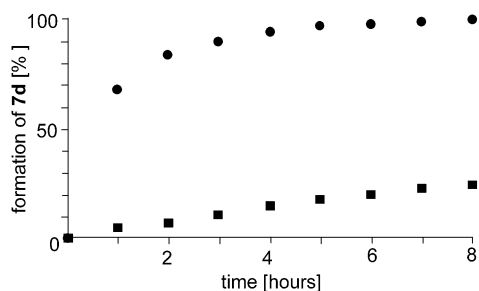
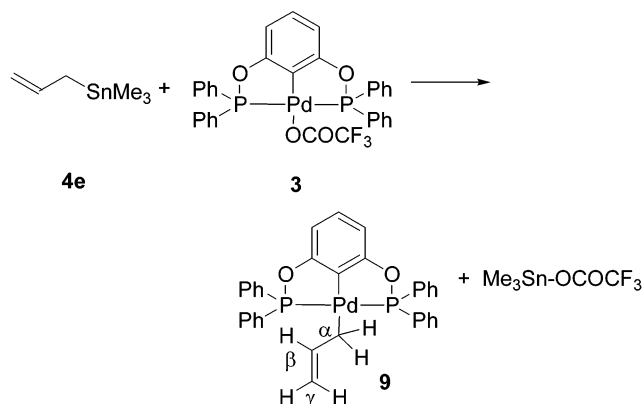


**Figure 1.** Formation of **7d** in the reaction of **4a** and **5d** (cf. entries 10 and 11) catalyzed by pincer complexes **2a** (■) and **3** (●) in  $\text{CDCl}_3$  at 25 °C.

**Scheme 4.** Formation of  $\eta^1$ -Allylpalladium Complex **9** by Transmetalation of Allylstannane **4e** with Pincer Complex **3**



with **4d** could be performed with catalyst **3** (entry 25), while this reaction is extremely slow with catalysts **1a** and **2a** under the same conditions.

We have monitored the catalytic reaction of **4a** with **5d** by  $^1\text{H}$  NMR spectroscopy at 25 °C (Figure 1). The diagram in Figure 1 clearly indicates that the rate of formation of **7d** is considerably higher with trifluoroacetate complex catalyst **3** than with chloro complex **2a**. This experiment confirms the above findings that pincer complex **3** is a formidable catalyst for the electrophilic substitution of allylstannanes.

### 3. Mechanistic Aspects

It is well-known that palladium(II) species readily undergo transmetalation with allylstannanes to form allylpalladium complexes. Transmetalation of (mono)allylpalladium complexes with allylstannane derivatives gives bisallylpalladium complexes, which subsequently react with electrophiles (Scheme 1).<sup>3,13</sup> Palladium–pincer complexes have been reported to undergo transmetalation with organometallic reagents including organostannanes.<sup>33–35</sup> For example, Cotter et al.<sup>33</sup> have shown that 2-furylstannane undergoes tin-to-palladium transmetalation with the triflate salt of **2**. Therefore, it is reasonable to assume that the first step of the studied reaction (Scheme 3) is transmetalation of the allylstannane (**4**) with the pincer complex catalyst (**1–3**) to give an  $\eta^1$ -allyl-coordinated pincer species (Scheme 4).

**Reactive Intermediate of the Reaction.** Our previous studies have shown that pincer complexes **1c** and **2b** react with

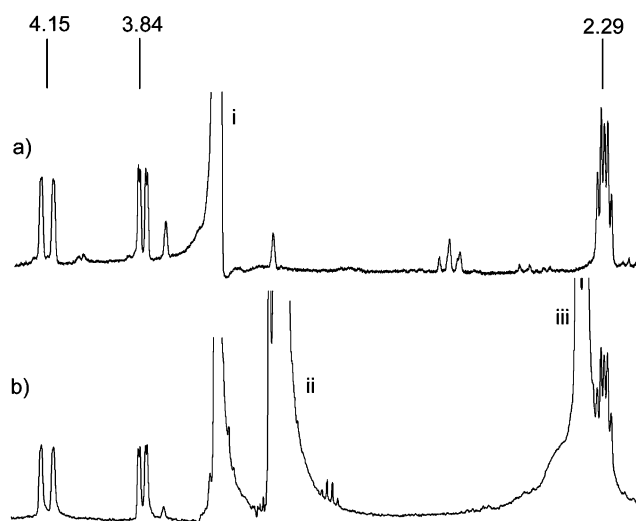
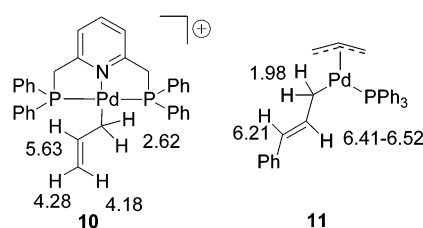


**Figure 2.** (a)  $^1\text{H}$  NMR spectrum of the reaction of complex **3** with allylstannane **4e**. (b)  $^1\text{H}$  NMR spectrum of the reaction of complex **3** with allylmagnesium bromide. Both reactions were conducted in  $\text{THF-}d_8$  (i,  $\text{THF-}d_8$ ; ii, ether; iii,  $\text{CH}_2\text{-MgBr}$ ). The shift values are given in parts per million.

**Chart 2.**  $^1\text{H}$  NMR Shift Values (in ppm) Reported for  $\eta^1$ -Allylpalladium Complexes Analogous to **9**.<sup>36,37</sup>



allylstannanes **4a** and **4e** even in the absence of aldehydes.<sup>19</sup> Monitoring of this reaction with  $^1\text{H}$  NMR spectroscopy revealed formation of propene from the allylstannane substrate. We supposed that the reaction involved transmetalation of the allylstannanes with palladium; however, the  $\eta^1$ -allylpalladium intermediate formed probably instantaneously reacted with traces of water present in the reaction mixture to give propene.

However, when a similar reaction was carried out with complex **3** and allyltrimethylstannane **4e** in dry  $\text{THF-}d_8$ , a number of relevant peaks between 2 and 5 ppm could be observed in the  $^1\text{H}$  NMR spectrum of the process (Scheme 4 and Figure 2a). One of these peaks appeared at 2.29 ppm as a doublet of triplets with coupling constants of 8.8 Hz ( $^3J_{\text{HH}}$ ) and 5.1 Hz ( $J_{\text{HP}}$ ). This shift value and coupling pattern are characteristic for the  $\alpha$ -protons of the  $\eta^1$ -allyl moiety in analogous pincer complexes (cf. Scheme 4 and Chart 2). For example, this proton resonates at 2.62 ppm with the same coupling pattern (dt,  $^3J_{\text{HH}} = 8.4$  Hz,  $J_{\text{HP}} = 5.3$  Hz) in complex **10** reported by Osborn and co-workers.<sup>36</sup> The resonance value for the  $\alpha$ -proton in **9** (2.29 ppm) is also in the range of NMR shifts reported for similar complexes (Chart 2) such as **10**<sup>36</sup> (2.62 ppm) and **11**<sup>37</sup> (1.98 ppm). Two other shift values at 4.15 and 3.84 ppm are also of great interest, since these shifts can be assigned to the  $\gamma$ -protons of the  $\eta^1$  moiety of **9**. The shift values are again very close to the  $\gamma$ -proton shifts reported for complex **10** (Chart 2).

To confirm the above  $^1\text{H}$  NMR shift assignments, we have carried out a control experiment. This experiment involved

(33) Cotter, W. D.; Barbour, L.; McNamara, K. L.; Hechter, R.; Lachicotte, R. *J. Am. Chem. Soc.* **1998**, *120*, 11016.

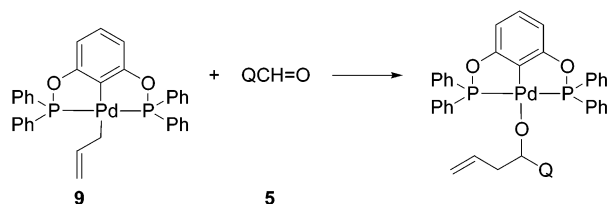
(34) Ohff, M.; Ohff, A.; Boom, M. E. v. d.; Milstein, D. *J. Am. Chem. Soc.* **1997**, *119*, 11687.

(35) Rimml, H. Thesis, ETH, Zürich, Switzerland, 1984.

(36) Barloy, L.; Ramdeehul, S.; Osborn, J. A.; Carloti, C.; Taulelle, F.; Cian, A. D.; Fischer, J. *Eur. J. Inorg. Chem.* **2000**, 2523.

(37) Kuhn, O.; Mayr, H. *Angew. Chem., Int. Ed.* **1999**, *38*, 343.

**Scheme 5.** Allyl Group Transfer from Complex **9** to the Aldehyde Electrophile



reaction of allylmagnesium bromide in place of **4e** with pincer complex **3**. It is well-known that the allyl Grignard reagents are much more reactive organometallic substrates than allylstannanes, and therefore these reagents instantaneously transmetalate with palladium(II) species including allylpalladium complexes.<sup>13,15,38</sup> Indeed, the same characteristic peaks at 2.29, 3.84, and 4.15 ppm appeared in the <sup>1</sup>H NMR spectrum of the reaction of allylmagnesium bromide with **3** (Figure 2b) as for the stoichiometric process of allylstannane **4e** with complex **3** (Figure 2a). Accordingly, we conclude that the stoichiometric reaction of **4e** with pincer complex **3** leads to  $\eta^1$ -allylpalladium pincer complex **9**, which we consider as the reactive intermediate of the studied catalytic electrophilic substitution (Scheme 3).

The above stoichiometric reaction (Scheme 4) can also be performed with allyltributylstannane **4a**. However, in the presence of a large excess of allylstannane **4a** the **9**:**3** ratio was only 0.18, which was remained unchanged in a longer period of time. On the other hand, when allyltrimethylstannane **4e** was employed (Figure 2a), the **9**:**3** ratio became considerably higher, up to 0.56. These observations indicate that under catalytic conditions the active catalyst **9** is generated in a lower concentration from allyltributylstannane derivatives than from allyltrimethylstannane substrates. This also explains the lower reactivity of allyltributylstannanes compared to allyltrimethylstannanes in the catalytic reactions.

**DFT Modeling of the Electrophilic Attack.** The key step of the catalytic reaction is obviously the coupling between the allyl moiety of the  $\eta^1$ -allyl complex (such as **9**) with aldehydes and imine electrophiles (Scheme 5). A peculiar feature of this reaction step is that only a single coordination site on palladium is available for the entire process. Thus, rationalization of the mechanism of the electrophilic attack on the  $\eta^1$ -allyl moiety of **9** (and its analogues) requires an explicit knowledge about the transition-state (TS) structure and the activation energy of the reaction. Therefore, we carried out density functional theory (DFT) calculations for the most important ground-state (GS) and TS structures of the process.

All geometries (**12** and **13**) were fully optimized by employing a Becke-type<sup>39</sup> three-parameter density functional model B3PW91 (Figure 3) with a double- $\zeta$ (DZ)+P basis constructed from the LANL2DZ basis<sup>40–42</sup> by adding one set of d-polarization functions to the heavy atoms (exponents: C, 0.63; O, 1.154; P, 0.34) and one set of diffuse d-functions on palladium (exponent 0.0628). All calculations have been carried out by employing the Gaussian98 program package.<sup>43</sup>

(38) Henc, B.; Jolly, P. W.; Salz, R.; Wilke, G.; Benn, R.; Hoffmann, E. G.; Mynott, R.; Schroth, G.; Seevogel, K.; Sekutowski, J. C.; Krüger, C. *J. Organomet. Chem.* **1980**, *191*, 425.

(39) Becke, A. D. *J. Chem. Phys.* **1993**, *98*, 5648.

(40) Dunning, T. H.; Hay, P. J. *Modern Theoretical Chemistry*; Plenum: New York, 1977; Vol. 3.

(41) Hay, P. J.; Wadt, W. R. *J. Chem. Phys.* **1985**, *82*, 270.

(42) Hay, P. J.; Wadt, W. R. *J. Chem. Phys.* **1985**, *82*, 299.

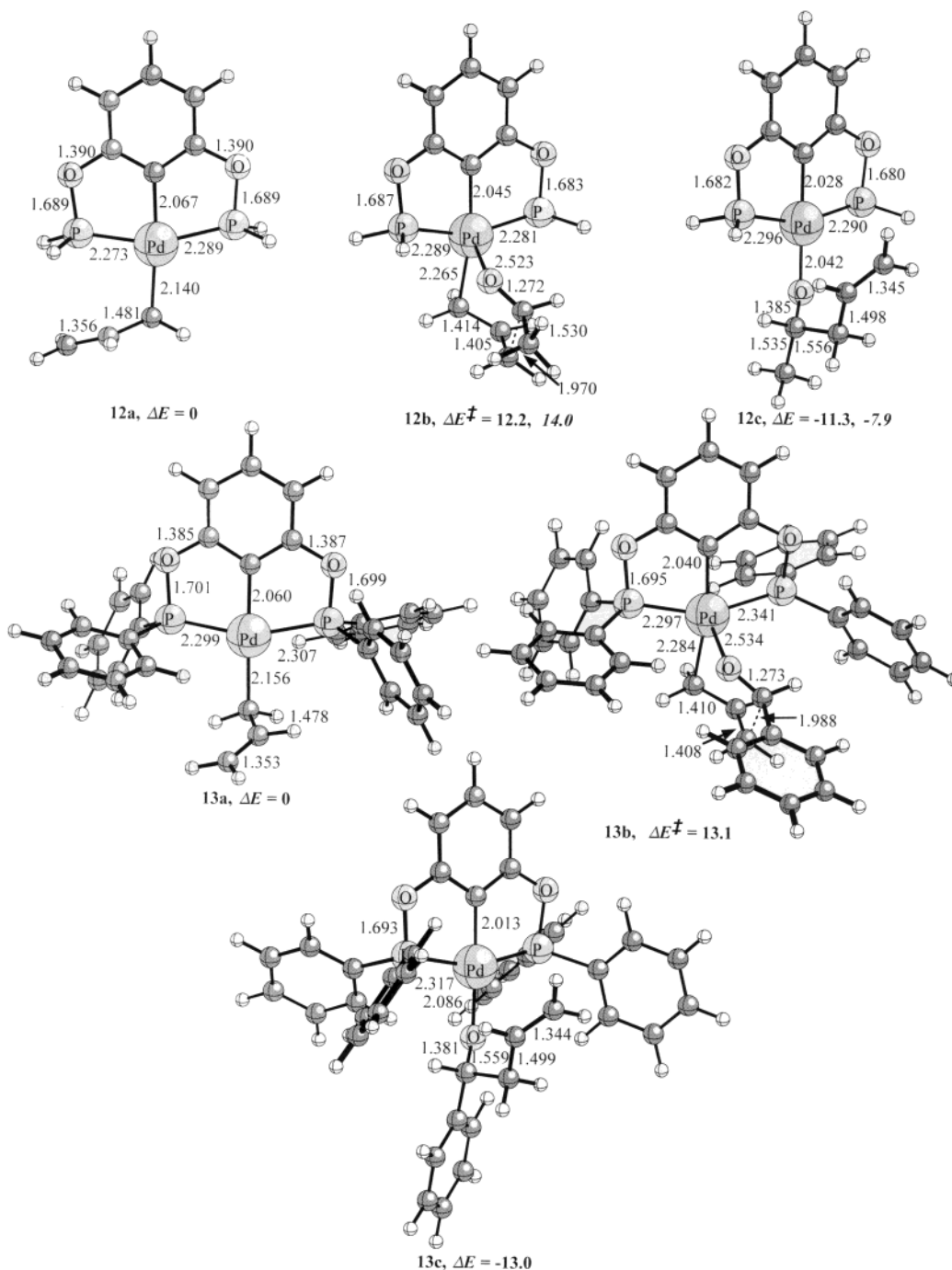
Species **12a–c** involve simplified models for the pincer ligand of **3** in which the phenyl groups are replaced by hydrogen atoms. In these calculations the benzaldehyde electrophile (**5a**) was approximated by an acetaldehyde molecule. The  $\eta^1$ -allyl species **12a** represents a minimum on the potential energy surface (PES) according to the vibrational analysis. The ligating atoms on palladium are in a square planar arrangement with a strong Pd–P coordination.

Complex **12b** was characterized as a TS structure, as its vibrational analysis gave only one imaginary frequency. The transition vector corresponds to the bond formation between the  $\gamma$ -terminus of the  $\eta^1$ -allyl moiety and the carbonyl carbon of acetaldehyde. The activation energy is only 12.2 kcal mol<sup>-1</sup> (the zero-point vibration corrected value is 14.0 kcal mol<sup>-1</sup>), which is similar to the activation barrier of these types of electrophilic attacks on bisallylpalladium complexes (10–15 kcal mol<sup>-1</sup>).<sup>8,12,14</sup>

In **12b** the  $\eta^1$ -allyl moiety, the carbonyl group, and the palladium atom form a cyclic six-membered ring structure with distinct equatorial and axial positions. This also requires that the  $\alpha$ -carbon atom of the allyl group and the oxygen of the aldehyde share a single coordination site on palladium. Thus the tridentate pincer-type ligation remains largely unaffected in the TS structure. This is also indicated by the fact that the strong Pd–P coordination is still maintained. As one goes from GS **12a** to TS structure **12b**, the Pd–P bond is changed by only 0.02 Å. The vibrational analysis of the product complex **12c** gave only real frequencies, indicating that it is a minimum on the PES. Formation of **12c** from **12a** is exoenergetic with 11.3 kcal mol<sup>-1</sup> (7.9 kcal mol<sup>-1</sup> with ZPV correction). In this complex the oxygen of the homoallyl product is coordinated to palladium, while the carbon–carbon double bond is uncoordinated.

The above DFT calculations with model systems **12a–c** indicate that the electrophilic substitution of the  $\eta^1$ -allyl moiety occurs readily with a low activation barrier. However, bulky phenyl substituents on the phosphorus atoms in the rigid firmly tricoordinated pincer ligand can be involved in destabilizing steric interactions with the substituents of the aldehyde component. These interactions can considerably increase the activation energy of the reaction and change the TS geometry. Therefore, we undertook theoretical studies for the realistic species **13a–c**, including phenyl groups on the pincer ligands and on the aldehyde substrate. As one goes from model complex **12a** to complex **13a**, the allyl group is rotated by about 90° to avoid the steric interactions with the phenyl groups of the pincer ligand. Otherwise, the geometrical parameters describing the allyl–metal and the Pd–P bonding are almost identical. The activation energy of the electrophilic attack by benzaldehyde on **13a** is 13.1 kcal mol<sup>-1</sup> (**13b**), which is only 0.9 kcal mol<sup>-1</sup> higher than the activation energy obtained for the model systems

(43) Frisch, M. J.; Trucks, G. W.; Schlegel, H. B.; Scuseria, G. E.; Robb, M. A.; Cheeseman, J. R.; Zakrzewski, V. G.; Montgomery, J. A.; Stratmann, R. E.; Burant, J. C.; Dapprich, S.; Millam, J. M.; Daniels, A. D.; Kudin, K. N.; Strain, M. C.; Farkas, O.; Tomasi, J.; Barone, V.; Cossi, M.; Cammi, R.; Mennucci, B.; Pomelli, C.; Adamo, C.; Clifford, S.; Ochterski, J.; Petersson, G. A.; Ayala, P. Y.; Q. Cui; Morokuma, K.; Malick, D. K.; Rabuck, A. D.; Raghavachari, K.; Foresman, J. B.; Cioslowski, J.; Ortiz, J. V.; Stefanov, B. B.; Liu, G.; Liashenko, A.; Piskorz, P.; Komaromi, I.; Gomperts, R.; Martin, R. L.; Fox, D. J.; Keith, T.; Al-Laham, M. A.; Peng, C. Y.; A. Nanayakkara; Gonzalez, C.; Challacombe, M.; Gill, P. M. W.; Johnson, B.; Chen, W.; Wong, M. W.; Andres, J. L.; Gonzalez, C.; Head-Gordon, M.; Replogle, E. S.; Pople, J. A. *Gaussian 98*; Gaussian, Inc.: Pittsburgh, PA, 1998.

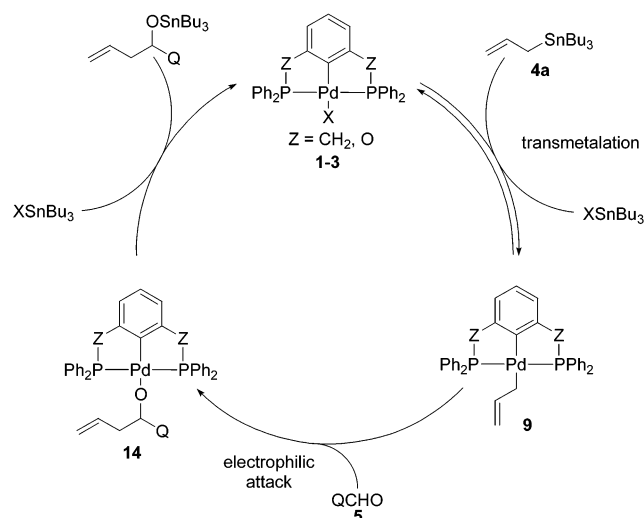
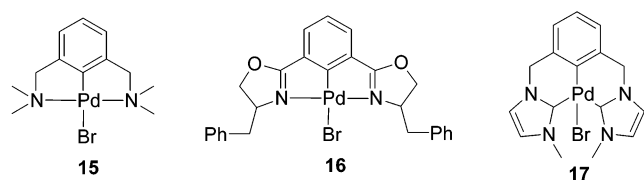


**Figure 3.** B3PW91/LANL2DZ+P optimized structures occurring in the electrophilic attack on the allyl moiety. The bond lengths are given in angstroms. The zero-point vibration corrected energies are shown in italic type; all energies are given in kilocalories per mole.

(**12a** → **12b**). Furthermore, the reaction also proceeds through a six-membered cyclic transition state (**13b**) and the geometry of the TS structures **13b** and **12b** is very similar. The reaction is exoenergetic with 13.0 kcal mol<sup>-1</sup> (**13c**), which compares well to the energetic features of the model reaction (12.2 kcal mol<sup>-1</sup>). Because of the large size of **13a–c**, the vibrational analysis is computationally prohibitive. However, the close resemblance between the corresponding species of **12a–c** and **13a–c** indicates that **13a** and **13c** are GS structures and **13b** is a TS structure. Accordingly, it can be concluded that the steric effects of the phenyl substituents of the pincer ligand and the substituents of the aldehyde component has a relatively weak

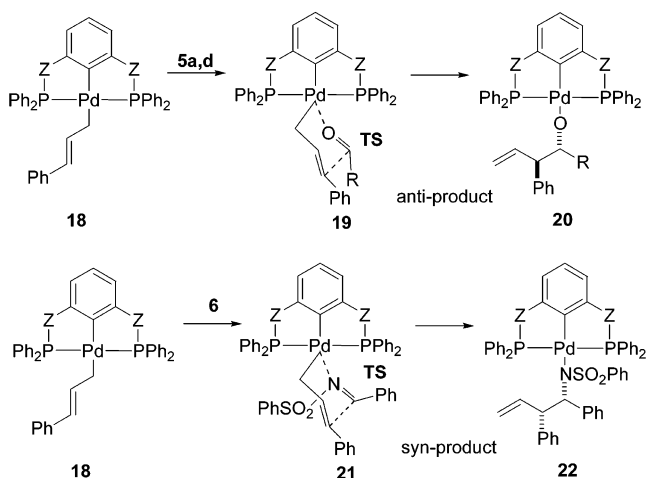
effect on the energetic features and on the TS geometry of the electrophilic attack.

**Catalytic Cycle of the Reaction.** On the basis of the results of the stoichiometric reaction of **3** with allylstannane **4e** (Scheme 4), the introducing step of the catalytic reaction is the transmetalation of the allylstannane substrate with the pincer complex catalyst (Scheme 6). The stoichiometric reactions indicate that this transmetalation is an equilibrium process, since only a certain portion of the pincer complex **3** is converted to **9** even in the presence of a large excess of allylstannane (**4a** or **4e**). Therefore, electronic and steric effects shifting the equilibrium to formation of the η<sup>1</sup>-allyl complex **9** are particularly important

**Scheme 6.** Catalytic Cycle of the Pincer Complex-Catalyzed Electrophilic Substitution Reaction**Chart 3.** Pincer Complexes with Low Catalytic Activity in the Electrophilic Substitution Reactions

factors to increase the rate of the catalytic transformation. Weakly coordinating counterions, such as trifluoroacetate (**3**), acetate (**1b**), and tetrafluoroborate (**1c** and **2b**), can be much more easily replaced with the allyl group than the chloride ion (**1a** and **2a**), which explains the high catalytic activity of **3** (**1b,c**) compared to **1a** and **2a**. In the transmetalation step, formally an allyl anion is transferred from **4a** to the pincer complex, and thus formation of **9** is thermodynamically not preferred when the electron density on palladium is too high. A high electron density on palladium can be generated by employment of  $\sigma$ -donor pincer ligands. Therefore, we have also investigated the catalytic activity of NCN complexes **15**<sup>25</sup> and **16**<sup>44</sup> and carbene complex **17** (Chart 3).<sup>45</sup> All three complexes exhibited low catalytic activity in the electrophilic substitution reactions, which probably can be due to the slow transmetalation step. As mentioned above, the steric and electronic features of the allylstannane substrate also influence the transmetalation. For example, allyltrimethylstannanes (**4b** and **4c**) are more reactive than their tributyl-substituted counterparts (e.g., **4a** and **4d**) in the catalytic reaction.

The electrophilic attack is probably the most important reaction step since it determines the regio- and stereoselectivity of the catalytic process. According to the above DFT studies, PCP complex **9** readily undergoes electrophilic attack with aldehydes (Scheme 5 and Figure 3). However, the electrophilic attack and the transmetalation step have opposite electron demands. In intermediate **9** a high electron density on palladium increases the nucleophilic character of the  $\eta^1$ -allyl moiety. On

**Scheme 7.** Rationalization of the Stereoselectivity of the Catalytic Transformation

the other hand, formation of complex **9** is facilitated by a low electron density on palladium (vide supra). Therefore, a careful consideration of the electronic effects of the pincer ligands is necessary to obtain a catalyst that shows high reactivity in both the transmetalation step and the electrophilic attack of the catalytic cycle. Pincer complexes **1–3** represent electronically well-balanced catalysts working equally well in both reaction steps. On the other hand, pincer complexes **15–17** (Chart 3) bearing an  $\eta^1$ -allyl ligand are expected to undergo a facile electrophilic attack; however, formation of these species by transmetalation from allylstannane is probably very slow.

The regioselectivity of the reaction (entries 19–26) can be explained by the substituent effects of the alkyl and aryl groups on the stability of  $\eta^1$ -allyl moieties. Our previous studies have clearly shown that the terminally substituted  $\eta^1$ -allyl complexes are more stable when the alkyl or aryl substituents are attached at the  $\gamma$ -terminus of the allyl moiety.<sup>9–12,14,18,19</sup> Since the electrophilic attack also occurs at the  $\gamma$ -position of the  $\eta^1$ -allyl moiety, the catalytic reaction affords the branched allyl isomer.

Cinnamylstannane **4b**, comprising a bulky phenyl substituent, reacted with high stereoselectivity (entries 19–22 and 26). Interestingly, the major stereoisomer with aldehydes **5a**, **5d**, and **5g** is the anti isomer, while the reaction with sulfonimine **6** affords mainly the syn diastereomer. The DFT calculations clearly show that the electrophilic attack proceeds through a six-membered cyclic TS, in which the allylic terminal substituents and the substituent of the aldehyde component occupy distinct axial and equatorial positions (**12b** and **13b**). In the calculated structures the orientation of the aldehyde molecules renders their substituents (Me in **12b** and Ph in **13b**) to an equatorial position. Considering that the trans geometry represents the most stable form for the cinnamyl moiety (**18**, Scheme 7), the phenyl substituent will also occupy an equatorial position in the TS structure (**19**). Thus in the most stable TS structure the bulky substituents are in a trans-diequatorial arrangement over the developing carbon–carbon bond, which leads to trans-diastereomer **20**. A similar model was employed to explain the stereoselectivity of the electrophilic attack via bisallylpalladium intermediates.<sup>12</sup> When crotylstannane **4c,d** is used, the level of the stereoselectivity is determined by the steric effects of the methyl substituent in the allyl moiety. Equal formation of syn and anti diastereomers (entries 23 and 24) can be ascribed to the small size of the allylic methyl substituent.

(44) Denmark, S. E.; Stavenger, R. A.; Faucher, A.-M.; Edwards, J. P. *J. Org. Chem.* **1997**, *62*, 3375.

(45) Gründemann, S.; Albrecht, M.; Loch, J. A.; Faller, J. W.; Crabtree, R. H. *Organometallics* **2001**, *20*, 5485.



The stereoselectivity in the reaction of **4b** with **6** (entry 26) is strongly influenced by the trans geometry of the phenylsulfonyl and phenyl groups across the carbon–nitrogen double bond in **6**. Because of this geometry, the lone pair on nitrogen (interacting with palladium) and the phenyl group are in a cis arrangement. Furthermore, it is reasonable to assume that in the TS structure **21** the close vicinity between the palladium atom and the sulfonyl group will be avoided. As a consequence, the preferred orientation of **6** in TS structure **21** renders the phenyl group to an axial position. Since the allylic phenyl group is in an equatorial position, this model predicts formation of the syn diastereomer **22**. It is interesting to note that a similar syn diastereoselectivity was reported for the formation of **8b** from **6** and cinnamyl bromide in indium- and zinc-mediated reactions.<sup>31</sup>

The theoretical calculations have shown that the electrophilic attack results in an alkoxide-coordinated homoallylic alcohol (**12c** and **13c**) as product. Under catalytic conditions these complexes (such as **14**) may undergo ligand exchange with the organotin salts formed in the transmetalation to give the final product and to regenerate the catalyst (Scheme 6). This reaction probably easily occurs due to the well-known low coordination ability of the alkoxides to palladium.

#### 4. Conclusions

In this study we have shown that palladium pincer complexes are formidable catalysts for electrophilic substitution of allylstannanes. Application of this procedure eliminates the side reactions occurring in the same catalytic transformations via bisallylpalladium intermediates. It was shown that complex **3** with weakly coordinating trifluoroacetate counterion has a remarkably high catalytic reactivity and stability under the applied catalytic conditions, and therefore it can be used for allylation of a broad variety of electrophiles. Complexes **1a** and **2a** are also robust catalysts; however, they are inferior to **3** in the studied electrophilic substitution reactions.

We have identified the active catalytic intermediate of the reaction, which is an  $\eta^1$ -allyl-coordinated pincer complex (**9**) formed by transmetalation from allylstannane and the pincer catalyst. Theoretical calculations indicate that the electrophilic attack proceeds with a low activation barrier on the  $\gamma$ -position of the  $\eta^1$ -allyl moiety of the active intermediate (**9**). The electrophilic attack takes place via a six-membered cyclic TS structure. The activation energy and the TS geometry are only slightly affected by the steric interactions between the bulky phenyl groups on the pincer ligand and the aldehyde substrate. The regio- and stereoselectivity of the reaction can be rationalized on the basis of the calculated TS geometry of the reaction.

It was found that the catalyst activity is determined by the ligand effects on the transmetalation step and on the electrophilic substitution step of the catalytic process. Since these steps have an opposite electron demand, PCP-type complexes are expected to show the highest activity in electrophilic substitution reactions. Furthermore, weakly coordinating counterions (such as trifluoroacetate, acetate, and borontetrafluoride) on palladium facilitate the transmetalation step, and therefore increase the catalytic activity of the applied pincer complex.

#### 5. Experimental Section

The NMR spectra were recorded on a Varian 400 MHz NMR spectrometer. The chemical shifts (ppm) are obtained by use of residual solvent as internal standard in <sup>1</sup>H NMR (THF-*d*<sub>8</sub>, 3.58 ppm) and phosphoric acid in <sup>31</sup>P NMR measurements. Merck silica gel 60 (230–400 mesh) was used for chromatography. All reactions were performed under an atmosphere of argon by standard manifold techniques. The solvents were carefully dried and distilled prior to use.

**Palladium-Catalyzed Allylation of Aldehydes by Pincer Complex Catalysts.** A mixture of the appropriate catalyst (0.007 mmol, 5 mol %) and aldehyde **5** (0.15 mmol) was dissolved in the corresponding solvent: in DMF (500  $\mu$ L) for catalyst **1a** and in THF for **2a** (500  $\mu$ L) and **3** (250  $\mu$ L). Subsequently, allylstannane **4** (0.18 mmol) was added to this mixture at room temperature. The reaction mixture was then stirred at the allotted temperatures and times listed in Table 1. Thereafter the reaction mixture with DMF as solvent (**1a**) was diluted with water and extracted with ether, while the reaction mixtures with THF as solvent (**2a** and **3**) were evaporated. The crude products were purified by silica gel column chromatography with pentane/ethyl acetate as eluent. The NMR data obtained for products **7** and **8** are in agreement with the corresponding literature values.<sup>28,30,31,46</sup>

**Comparison of the Catalytic Activity of 2a and 3 (Figure 1).** The appropriate pincer complex (0.0075 mmol) and **5d** (22.7 mg, 0.15 mmol) were dissolved in CDCl<sub>3</sub> (500  $\mu$ L) and transferred to an NMR tube. To this mixture was added allyltributylstannane **4a** (56  $\mu$ L, 0.18 mmol) at 0 °C. Then the reaction mixture was heated to 25 °C and the progress of the reaction was followed by <sup>1</sup>H NMR spectroscopy.

**Stoichiometric Reaction of Pincer Complex 3 with Allyltrimethylstannane 4e.** Pincer complex **3** (0.008 mmol) dissolved in dry THF-*d*<sub>8</sub> (600  $\mu$ L) was transferred into a carefully dried NMR tube. To this solution was added allyltrimethylstannane **4e** (0.2 mmol) at –10 °C. After homogenization, a clear yellow reaction mixture was obtained, which was studied by <sup>1</sup>H and <sup>31</sup>P NMR spectroscopy at –10 °C. The shift values for complex **9** were determined from the NMR spectra of this reaction mixture. The only exception is the <sup>1</sup>H NMR shift at 5.91 ppm, which overlaps with the H<sub>2</sub> resonance of **4e**. This shift value was determined from the reaction mixture of **3** with allylmagnesium-bromide (see below). <sup>1</sup>H NMR (see also Figure 2a) in THF-*d*<sub>8</sub>:  $\delta$  7.76 (m, 8H), 7.52 (m, 12H), 6.97 (t, *J* = 8.0 Hz, 1H), 6.66 (d, *J* = 8.0 Hz, 2H), 5.91 (m, 1H), 4.15 (d, *J* = 16.5 Hz, 1H), 3.84 (dd, *J* = 10.0 and 2.2 Hz, 1H) 2.29 (dt, *J* = 8.8 and 5.1 Hz, 1H). <sup>31</sup>P NMR:  $\delta$  147.1

**Stoichiometric Reaction of Pincer Complex 3 with Allylmagnesium Bromide.** The NMR tube charged with **3** (0.01 mmol) dissolved in THF-*d*<sub>8</sub> (500  $\mu$ L) was cooled to –10 °C. Thereafter, allylmagnesium bromide in THF-*d*<sub>8</sub> (200  $\mu$ L, 0.25 M, 0.05 mmol) was added and the reaction mixture was homogenized to give a yellow solution. The NMR shift values obtained for **9** in this experiment (Figure 2b) and in the experiment given above (Figure 2a) are identical.

**Acknowledgment.** This work was supported by the Swedish Natural Science Research Council (NFR). The calculations were done at the IBM SP2 parallel computer facility of the Paralleldatorcentrum (PDC) at the Royal Institute of Technology, Sweden. We thank the PDC for a generous allotment of computer time.

JA049357J

(46) Jones, P.; Knochel, P. *J. Org. Chem.* **1999**, *64*, 186.